The critical end point in QCD

R. V. Gavai and Sourendu Gupta [a*]

[a]Department of Theoretical Physics,
Tata Institute of Fundamental Research,
Homi Bhabha Road, Mumbai 400005, India

In this talk I present the logic behind, and examine the reliability of, estimates of the critical end point (CEP) of QCD using the Taylor expansion method.

1. The method and results

The global structure of the expected phase diagram of two flavour QCD is the following [1]. In the chiral limit of two flavour QCD, *i.e.*, when $m_\pi = 0$, one expects the chiral phase transition to occur at a critical point at finite temperature, T, and zero baryon chemical potential, μ_B. This critical point is expected to develop into a critical line in the plane of T and μ_B for $m_\pi = 0$, and turn into a line of first order transitions at a tricritical point. When $m_\pi \neq 0$, the structure changes dramatically. There is no critical line; rather there is a first order line ending in a critical end point (the CEP) in the Ising universality class at $T^*(m_\pi)$ and $\mu_B^*(m_\pi)$. With varying m_π the CEP traces out a "wing critical line" ending at the tricritical point. These considerations are based on symmetry arguments and universality, and hence are expected to be robust.

Direct verification of this picture involves lattice QCD computations in the chiral limit and finite chemical potential. Both are technically unfeasible at this time, the former due to chiral slowing down (computer time requirements diverge as $m_\pi \to 0$) and the latter due to the sign problem (Monte Carlo is impossible at finite μ_B). The strategy of [2] is not to prove or disprove this picture directly, but, by assuming this picture, to estimate $T^*(m_\pi)$ and $\mu_B^*(m_\pi)$.

This is done by making a Taylor expansion of the pressure around $\mu_B = 0$—

$$P(T,\mu_B) \equiv \left(\frac{T}{V}\right) \log Z(T,\mu_B) = P(T,0) + \sum_n \chi_B^n(T) \frac{\mu_B^n}{n!}. \tag{1}$$

CP symmetry of the problem reduces every odd coefficient to zero, hence the sum starts with the term in $n = 2$. This induces a series for the quark number susceptibility (QNS), which is the second derivative of the pressure with respect to μ_B, and the associated radius of convergence—

$$\frac{\chi(T,\mu_B)}{T^2} \equiv \frac{\partial^2 P(T,\mu_B)}{\partial \mu_B^2} = \sum_{n=0}^{\infty} \frac{T^{n-2}\chi_B^{n+2}(T)}{n!} \left(\frac{\mu_B}{T}\right)^n, \qquad \rho^{n+1} = \sqrt{\left|\frac{n! T^{-2}\chi_B^n(T)}{(n-2)!\chi_B^{n+2}(T)}\right|}. \tag{2}$$

*Talk presented by SG

We have used T to convert the series to one in the dimensionless variable μ_B/T. Since we use this expansion at fixed T, there is complete equivalence with the dimensional form. A notational convention used here is $\chi(T, \mu_B = 0) = \chi_B^2(T)$.

At the CEP this QNS is expected to diverge in the thermodynamic limit. Let ρ^* denote the limit of ρ^n as $n \to \infty$, evvaluated in the thermodynamic limit. Then, somewhere on the circle of radius $\rho^*(T)$ in the complex plane, we are assured of finding a singular point. If this singular point is on the real axis, then we have found the critical end point.

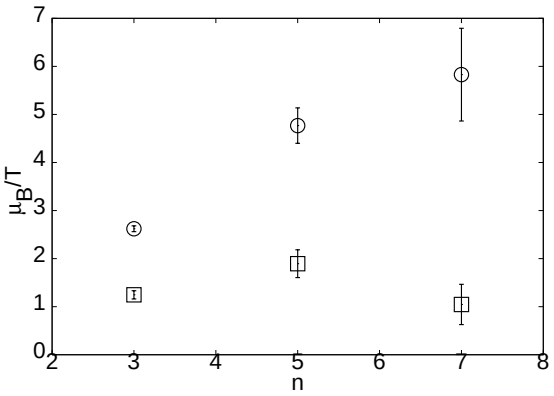

Figure 1. μ_B^n as a function of the order, n, for small ($Lm_\pi \simeq 3$, circles) and large ($Lm_\pi \simeq 9$, boxes) volumes at $T = 0.95T_c$.

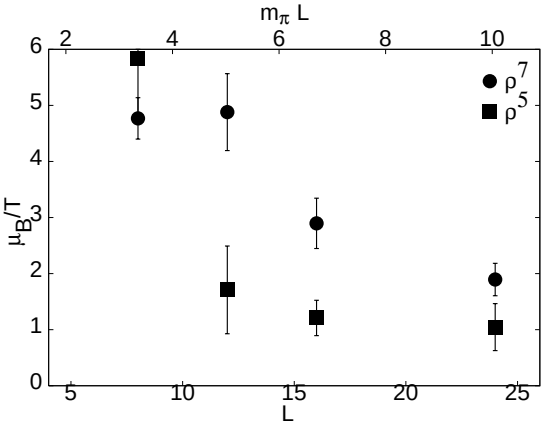

Figure 2. $\rho^{5,7}$ as a function of the lattice size, Lm_π at $T = 0.95T_c$.

One complication is that in a lattice computation one perforce uses finite spatial volumes— a cube with sides L. On finite volumes there is no true phase transition, so the limit of ρ^n as $n \to \infty$ must be infinite. One expects the sequence $\rho^n(T, L)$ to approach some value $\rho^*(T, L)$ for restricted values of n, before climbing to infinity. As L increases, the range of n for which this stable plateau in $\rho^n(T, L)$ is seen should increase and the plateau value, $\rho^*(T, L)$, should converge to the thermodynamic limit $\rho^*(T)$. In Figure 1 we show that $\rho^n(T, L = 3.3/m_\pi)$ increases continually with n, whereas a stable value is seen for $\rho^n(T, L = 10/m_\pi)$. In Figure 2 we show that $\rho^{5,7}(T, L)$ cross over from small to large volume behaviour at $Lm_\pi \geq 5$. The extrapolation from large volumes to the thermodynamic limit can be made using finite size scaling. In [2] this is performed assuming that the CEP is in the Ising universality class.

In [2] as T was lowered from a very high value, it was found that the radius of convergence decreased from a very large value to $\rho^* \approx T$. Oscillations in the sign of the non-linear susceptibilities (NLS, χ_B^n) indicated that the singularity was at complex ρ^*. On further lowering T it was found that all the series coefficients have positive sign (Figure 3), showing that the singularity moves to real ρ^*, allowing the identification of $T^*(m_\pi)$ and $\mu_B^*(m_\pi)$.

The technical part of the computation involves the choice of action. For the gauge fields,

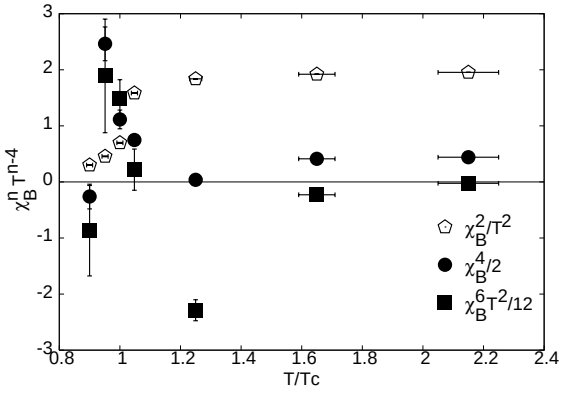

Figure 3. The temperature dependence of the successive NLS.

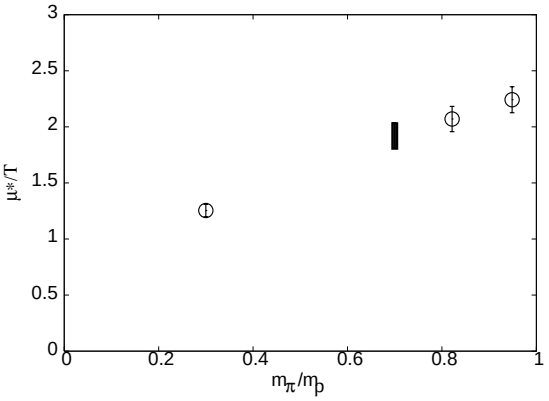

Figure 4. Variation of ρ^3 with m_π; the bar is data from [7].

we have taken the Wilson action and for the quarks we have two flavours of staggered quarks. Staggered quarks at finite chemical potential have many uncertainties at finite lattice spacing [3, 4]. Since the method of Taylor expansions uses only simulations at $\mu_B = 0$ [2, 7], they may give results which agree with those obtained by reweighting [5] or analytic continuation of simulations at imaginary μ_B [6] only in the continuum limit. At present there are no simulations with Wilson quarks.

The lattice simulations were carried out at lattice spacings $a = 1/4T$. The scale was set by the finite temperature crossover at T_c, giving $m_\rho/T_c = 5.4$. The quark mass was chosen such that $m_\pi/m_\rho = 0.31$ (compared to 0.18 in the real world). This agrees with the simulation parameters of [5, 6] but not with those of [7] which differ by having $m_\pi/m_\rho = 0.7$.

An exploratory study of the variation of the CEP with m_π/m_ρ can be performed in partially quenched QCD, *i.e.*, in QCD where the sea quark masses are allowed to be different from the valence quark masses. In such an exercise we found the radius of convergence to vary by large amounts. We show our results in Figure 4. It is interesting that the results of [7] are close to the curve generated by these computations, indicating that the apparent difference between [2] and [7] could largely be a matter of change in m_π.

2. Two technical points

A major question in lattice simulations is that of statistics. In [2] the measurements were taken on $N_{stat}^{bare}/(2\tau_{int}+1) = 50$–$200$ statistically independent configurations. Statistical independence is measured by the integrated autocorrelation time, τ_{int}. Since statistical errors change as $\sqrt{(2\tau_{int}+1)/N_{stat}^{bare}}$, increase of statistics by a factor of 4 could easily be offset if $\tau_{int} = 1$ instead of zero. Much more important is the statistics used in the estimator of fermion traces, which we shall discuss next.

2.1. Evaluating traces and their products

The Taylor expansion coefficients, the NLS χ_B^n, in eqs. (1,2) involve derivatives of the quark determinant, which become traces over quark loops. Traces of very large matrices are efficiently evaluated by the identity $\mathrm{T}r\, A = \mathrm{T}r\, AR$ where R is a stochastic representation of the identity matrix—

$$R = \frac{1}{2N_v} \sum_{i=1}^{N_v} |r_i\rangle \langle r_i| \stackrel{N_v \to \infty}{\longrightarrow} I, \tag{3}$$

the limit being obtained when $|r_i\rangle$ is one of a set of N_v vectors of complex numbers, each component drawn independently from a distribution with vanishing mean. Typically one has to evaluate traces as well as products of traces—

$$a_j = \frac{1}{2} \sum_{\alpha\beta} \sum_{i=1}^{N_v} A_{\alpha\beta} r_{i\,\alpha}^{j\,*} r_{i\,\beta}^{j}, \qquad p_n = \prod_{j=1}^{n} a_j, \qquad \overline{p_n} = \prod_j \mathrm{T}r\, A_j = \prod_j \left[\frac{1}{N_v} \sum_{i=1}^{N_v} a_j \right] = \prod_j \overline{a_j}, \tag{4}$$

where the factorisation of the average (denoted by a bar over the symbol) of p_n occurs when the different sets of random vectors r^j are independent. Here α and β are matrix indices. If the random vectors are drawn from a Gaussian distribution, then a_j is clearly a Gaussian distributed variable with mean $\overline{a_j} = \mathrm{T}r\, A_j$ and variance $\sigma_j^2 \propto 1/N_v$. Hence the product of traces is a product of independent Gaussian random variables.

A product of Gaussian random variables is not Gaussian. To prove this, consider $\delta_j = a_j - \overline{a_j}$, which is Gaussian distributed with zero mean, so $\langle \delta_j^2 \rangle = \sigma_j^2$ and $\langle \delta_j^4 \rangle = 3\sigma_j^4$, so that $[\delta_j^4] \equiv \langle \delta_j^4 \rangle - 3\langle \delta_j^2 \rangle = 0$, as must be true for a Gaussian. In that case, however, the product $d = \prod_{j=1}^n \delta_j$ has the property that

$$\langle d^2 \rangle = \prod_{j=1}^{n} \langle \delta_j^2 \rangle = \prod_{j=1}^{n} \sigma_j^2, \qquad \langle d^4 \rangle = \prod_{j=1}^{n} \langle \delta_j^4 \rangle = 3^n \prod_{j=1}^{n} \sigma_j^4, \qquad [d^4] = (3^n - 3) \prod_{j=1}^{n} \sigma_j^4 \neq 0, \tag{5}$$

where the factorisation of the expectation values follows from the independence of the δ_j's. Thus products of Gaussians are highly non-Gaussian.

Since the central limit theorem applies, estimators of $\overline{d}$ are still Gaussian distributed. It would seem that the fourth cumulant varies as $(3^n - 3)/N_v^{2n}$, and therefore the Gaussian is approached rapidly. In actuality the situation is worse, as one can check by reconstructing the distribution of $p_n = \prod_j (\overline{a_j} + \delta_j)$. We find that $[p_n^4]$ is dominated by the slowest falling term, which varies as n^2/N_v^2, rather than the most rapidly falling term $(3/N_v^2)^n$. It was found that $N_v \simeq 30$ are needed to control errors for $n = 2$ [3]. Consistent with this, $N_v \simeq 500$ are needed to control errors for $n = 8$ [2]. Conversely, using $N_v = 100$ for $n = 6$ [7] is equivalent to working with $N_v \simeq 10$ for $n = 2$.

2.2. Critical divergence

Since we analyze the series expansion of eq. (2) to estimate the critical end point shouldn't one be able to use the series to see critical divergence? In fact, the lack of such a divergence has been used as an argument for the absence of the critical end point in [7]. However, it has been known since the 1960's that the partial sum of the series expansion is generically perfectly smooth across the critical point as determined by the radius of convergence upto the same order.

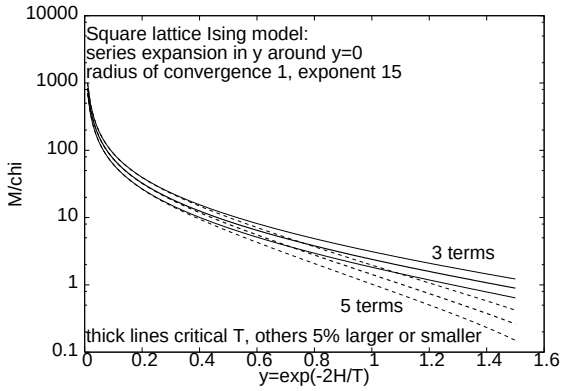

Figure 5. Partial series for the ratio m/χ. There is no hint of critical behaviour at $y = 1$.

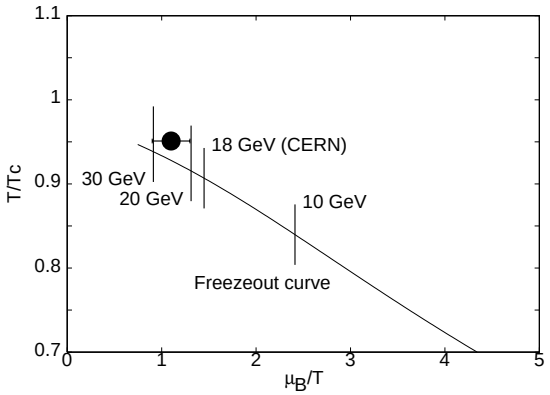

Figure 6. A comparison of the CEP obtained in [2] with the freezeout curve in heavy-ion collisions [9].

As an illustration I show results for the series expansion of the magnetic susceptibility, χ, of the two dimensional Ising model on a square lattice. The expansion is made in $y = \exp(-2H/T)$ around the point $y = 0$, where H is the magnetic field and T the temperature. This series has a radius of convergence unity. The exact ratio m/χ (where m is the magnetization) vanishes in the ordered phase. However, as shown in Figure 5, the ratio is perfectly smooth across $y = 0$.

One consequence of this realization is that the agreement of a series expansion of the pressure summed to low orders with any effective theory, for example, a resonance gas model, cannot be used to exclude the possibility of a critical end point.

3. Summary

There are four measures of reliability of lattice simulations of QCD—

1. the lattice spacing, a, which must be taken to zero, but in current computations is $1/4T$ [2, 5, 6, 7, 8]. The next generation of computations will reduce the lattice spacing by 33%.

2. the quark mass, which has to be tuned by fixing the pion mass or the ratio m_π/m_ρ. The physical value of this ratio is 0.18. In [2, 5, 6] this was taken be 0.31, in [7] it is 0.7 and in [8] it is the physical value.

3. the spatial size of the lattice, L, which must be taken to infinity through the process known as finite size scaling in order to obtain reliable results for thermodynamics. It was found that $Lm_\pi < 5$ gave rise to tremendous finite size distortions [2]. Only [2, 7] use lattices larger than this.

4. the statistical precision, $N_{stat}^{true} = \sqrt{N_{stat}^{bare}/(2\tau_{\rm int}+1)}$, where $N_{\rm stat}^{bare}$ is the number of configurations generated and τ_{int} is a measure of statistical independence called

the integrated autocorrelation time. When $\tau_{int} = 0$, the naive statistics actually represents the true statistics, but even the small value $\tau_{int} = 1$, causes the true statistics to be three times smaller than N_{stat}^{bare}. In [2] $N_{stat}^{true} = 50$–200 at all T, whereas no other simulation reports measurements of τ_{int}.

In addition, any computation of the expectation of products of fermion traces contains another measure of reliability. This is the number of vectors, N_v, used in evaluating the traces. Its crucial role is explained in Section 2.1.

The method of Taylor expansions can give reliable answers to questions about the QCD phase diagram once all these technical matters are under control. The critical end point can be determined in two steps—

1. Generate the series coefficients for the QNS in eq. (2) and evaluate the radius of convergence of the series.

2. When all the series coefficients have the same sign, the radius of convergence implies a singularity at real μ_B, which is the location of the CEP.

This works although the partially summed series for the pressure (eq. 1) or the QNS (eq. 2) are not expected to give the physical values of these quantities, as we show through examples in section 2.2. As a result, comparison of models, such as the resonance gas model, with the partial series sums is blind to the physics of the critical end point.

The CEP of QCD can be obtained from the results presented in [2], with $Lm_\pi > 5$, pion mass within 50% of the physical pion mass, and with good statistical control. The result is shown in Figure 6 superposed on the freezeout curve obtained in [9]. Computations at smaller lattice spacings would be very useful in checking the stability of this result.

REFERENCES

1. J. Berges and K. Rajagopal, Nucl. Phys., B 538 (1999) 215; M. A. Halasz *et al.*, Phys. Rev., D 58 (1998) 096007.
2. R. V. Gavai and S. Gupta, Phys. Rev., D 71 (2006) 114014.
3. R. V. Gavai and S. Gupta, Phys. Rev., D 68 (2003) 034506.
4. M. Golterman, Y. Shamir and B. Svetitsky, hep-lat/0602026.
5. Z. Fodor and S. Katz, J. H. E. P., 0203 (2002) 014.
6. P. de Forcrand and O. Philipsen, Nucl. Phys., B 642 (2002) 290.
7. C. Allton *et al.*, Phys. Rev., D 71 (2005) 054508.
8. Z. Fodor and S. Katz, J. H. E. P., 0404 (2004) 050.
9. J. Cleymans, J. Phys., G 30 (2004) S595, and private communication.